JOURNAL OF AIRCRAFT
Vol. 44, No. 6, November–December 2007

Assessment of Critical Fuel Configurations Using Robust Flutter Analysis

Sebastian Heinze*
Royal Institute of Technology, 100 44 Stockholm, Sweden

DOI: 10.2514/1.30500

An approach to assess critical fuel configurations using robust flutter analysis is presented. A realistic aircraft model is considered to demonstrate how an available finite element model can be adapted to easily apply robust flutter analysis with respect to structural variations such as fuel-level variations. The study shows that standard analysis tools can be used to efficiently generate the system data that are required to perform robust flutter analysis. The μ-k method is used to compute the worst-case flutter speed, and the corresponding worst-case fuel configuration is found. The main advantage of the proposed approach is that μ analysis guarantees robustness with respect to all possible fuel configurations represented by the tank model.

Introduction

TO CERTIFY new or modified aircraft, a large number of flutter analyses have to be performed to ensure that all configurations of the aircraft are free from flutter. All aerodynamic and structural variations have to be assessed; for example, mass variation due to fuel burn. Combining all possible variations, the number of configurations increases rapidly. Consequently, only a subset of all configurations can realistically be treated, meaning that the most critical configuration may not be detected.

In this paper, the possibility to use robust flutter analysis to ensure flutter stability for a range of different aircraft configurations is investigated. With this approach, a numerical model that depends on a set of bounded parameters defining the different configurations is developed, and a robust flutter analysis is performed to determine the flight condition in which some of the possible configurations becomes critical. Robust tools from the control community [1] are used to perform the robust flutter stability analysis. Robust flutter analysis has been the focus of research for some years, in which the structured singular value μ was considered to compute robust flutter bounds based on modeling uncertainties [2,3]. Studies specifically aiming at structural uncertainties and variations have been presented [4–6]. In the present study, the μ-k method [7–9] for robust flutter solutions is used for this purpose. The μ-k method extends standard frequency-domain flutter analysis to take model uncertainty into account and allows for reuse of existing flutter models and results.

In a previous study, the impact of a varying concentrated mass on the flutter speed of a simple wind-tunnel model was successfully treated with this approach [10]. This study focused on the influence of structural mode-shape variations on the robust flutter speed. The present study aims at demonstrating the same technique in the case of a high-fidelity aircraft model, in which an approach for modeling realistic fuel-level variations is presented, and robust analysis is used to assess critical fuel configurations. In addition, procedures to account for mode-shape perturbations due to structural variations are further investigated.

Presented as Paper 2279 at the 47th AIAA/ASME/ASCE/AHS/ASC Structures, Structural Dynamics, and Materials Conference, Newport, RI, 1–4 May 2006; received 23 February 2007; accepted for publication 3 June 2007.

*Ph.D. Student, Division of Flight Dynamics, Teknikringen 8. Member AIAA.

Aircraft Model

A generic subsonic aircraft with a wingspan of 17 m and an aspect ratio of 15.5 is considered to demonstrate the approach. The aircraft is a glider aircraft with geometric and structural properties that are similar to typical high-altitude long-endurance aircraft. Because the aircraft has been investigated in previous studies, a Nastran shell model of the structure was available [11,12]. Figure 1 shows the finite element discretization of the aircraft structure.

The model consists of approximately 12,000 grid points with a total of $n = 70,000$ degrees of freedom; 23,000 triangular and quadrilateral plate elements and some beam elements are used. Unlike the original glider aircraft, tanks were modeled in the wings and coupled to the structure using linear interpolation elements in Nastran. These elements couple inertial forces from the tank to the structure without contributing to the structural stiffness.

Approximately 2000 doublet-lattice panels representing the lifting surfaces were defined in Nastran and interpolated to the structure using thin-plate splines. Control surfaces were modeled to allow interaction between elastic modes and control-surface deflections. Because it turned out that the critical flutter mechanism is symmetric with respect to the aircraft symmetry plane, the rudder and antisymmetric aileron degrees of freedom were locked, to reduce the complexity of the model.

Modeling of Fuel Variation

A realistic fuel-tank geometry for the aircraft was defined as shown in Fig. 2, with the tanks being symmetric with respect to the x–z plane. Two different configurations were considered, denoted as configurations A and B, according to the figure. The simplest way to consider fuel variation in flutter analysis is to introduce a parameter that describes the fuel level and to perform flutter analyses for a set of different fuel levels. Using multiple parameters to model different fuel distributions would, however, increase the number of required flutter analyses significantly. Using an approach based on robust analysis, multiple parameters can be treated more efficiently. To demonstrate this, the tank was discretized as shown in the figure, in which a case with four tank elements is shown.

Each of the tank elements T_i was modeled as shown in Fig. 3. Note that it is essential to describe the mass variation as a polynomial function of some parametric variation δ. In the most simple case, the mass variation can be described as a linear function of the variation parameter. To obtain linearity in the present case, the tank boundaries for configuration A were simplified, as indicated in the figure. This reduces the complexity and size of the problem, as will be discussed later. Note that the simplified description may be improved by compensating for geometric approximations by modifying parameters such as the fuel density. In the present study, it was not considered necessary to compensate for the simplified geometry.

Fig. 1 Shell model of the aircraft.

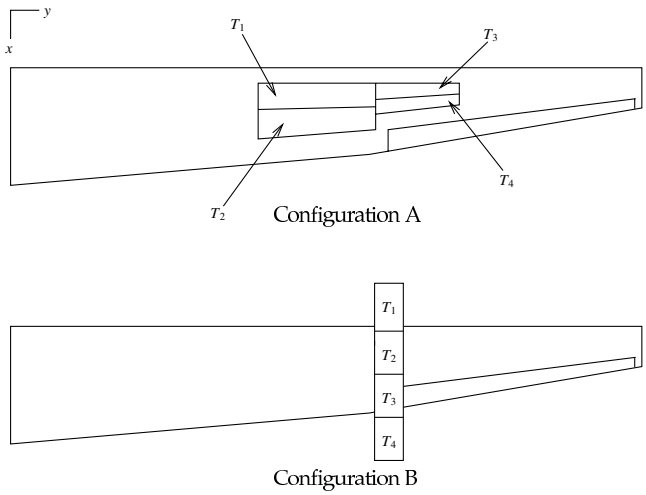

Fig. 2 Tank geometries and discretizations.

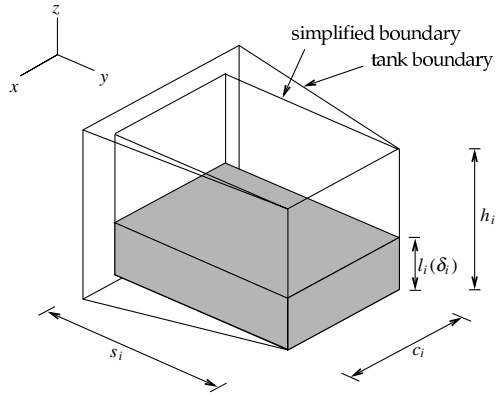

Fig. 3 Simplified tank element.

Using the notation defined in Fig. 3, the fuel level l_i and the fuel mass m_i within each element become

$$l_i = \left(\frac{\delta_i + 1}{2}\right) h_i \tag{1}$$

$$m_i = \left(\frac{\delta_i + 1}{2}\right) M_i \tag{2}$$

with $M_i = \rho_f s_i c_i h_i$ being the maximum fuel mass, where ρ_f is the fuel density, and s_i, c_i, and h_i are the tank element dimensions, as shown in the figure. The fuel level l_i in each of the tank elements T_i is represented by the parameter δ_i with $-1 \le \delta_i \le 1$, where $\delta_i = 1$ and $\delta_i = -1$ correspond to a full and empty tank, respectively. Using the simplified model, the mass moment of inertia around the center of mass of the fuel can be written as

$$I_{xx,i} = \frac{m_i(\delta_i)}{12}\left[l_i^2(\delta_i) + s_i^2\right] \tag{3}$$

$$I_{yy,i} = \frac{m_i(\delta_i)}{12}\left[c_i^2 + l_i^2(\delta_i)\right] \tag{4}$$

$$I_{zz,i} = \frac{m_i(\delta_i)}{12}\left(c_i^2 + s_i^2\right) \tag{5}$$

Because mass and fuel level depend linearly on δ_i, the mass moment of inertia depends on δ_i, δ_i^2, and δ_i^3. Note that both the mass and mass moment of inertia will contribute linearly to elements in the mass matrix of the finite element model. Therefore, the mass matrix also depends on the variation parameter to the third power. If fuel level and fuel mass depend on δ to some higher order, the order of the terms in the mass matrix will increase accordingly. Also note that there is no coupling between the different δ_i.

Varying Mass Matrix

To apply robust analysis, the mass variation must be posed in the form of a varying mass matrix that depends on some vector δ containing variation parameters δ_i. As noted earlier, the mass matrix can be written as

$$\boldsymbol{M}(\delta) = \boldsymbol{M}_0 + \sum_{i=1}^{r} \delta_i \boldsymbol{M}_{i1} + \delta_i^2 \boldsymbol{M}_{i2} + \delta_i^3 \boldsymbol{M}_{i3} \tag{6}$$

where r is the number of tank elements and $\boldsymbol{M}_{ij}$ are matrices to be determined. The matrix denoted as $\boldsymbol{M}_0$ corresponds to the mass matrix in which all δ_i equal zero, which means that all tank elements are half-filled. There are several ways to determine the matrices $\boldsymbol{M}_{ij}$. For simple mass variations with few nonzero elements in $\boldsymbol{M}_{ij}$, these matrices can be derived by hand. Because of a more complex variation of the mass matrix in the present case, Nastran was used to compute multiple $\boldsymbol{M}(\delta)$ for a set of δ. Based on Eq. (6), the matrices $\boldsymbol{M}_{ij}$ were then determined by

$$\boldsymbol{M}_{i1} = -\tfrac{1}{2}\boldsymbol{M}_{\delta_i=1} + \tfrac{8}{3}\boldsymbol{M}_{\delta_i=0.5} - \tfrac{1}{6}\boldsymbol{M}_{\delta_i=-1} - 2\boldsymbol{M}_0 \tag{7}$$

$$\boldsymbol{M}_{i2} = \tfrac{1}{2}\boldsymbol{M}_{\delta_i=1} + \tfrac{1}{2}\boldsymbol{M}_{\delta_i=1} - \boldsymbol{M}_0 \tag{8}$$

$$\boldsymbol{M}_{i3} = \boldsymbol{M}_{\delta_i=1} - \tfrac{8}{3}\boldsymbol{M}_{\delta_i=0.5} - \tfrac{1}{3}\boldsymbol{M}_{\delta_i=-1} + 2\boldsymbol{M}_0 \tag{9}$$

Note that the variation of δ_i is performed with $\delta_j = 0$ for all $j \ne i$. Thus, $(3r + 1)$ Nastran evaluations have to be performed to obtain all $\boldsymbol{M}_{ij}$ and $\boldsymbol{M}_0$. Note that Nastran is used to assemble the structural matrices of the system and to reduce the matrices by applying boundary conditions and multipoint constraints, but not to perform any analysis. Both nominal and robust flutter analysis were performed using Matlab and the Matlab μ-Analysis and Synthesis Toolbox [13].

Linear Fractional Transformation Form of Mass Matrix

To comply with the notation used in previous work on robust flutter analysis [7,10], Eq. (6) can be rewritten according to

$$\boldsymbol{M}(\delta) = \boldsymbol{M}_0 + \boldsymbol{M}_{L1}\Delta_M\boldsymbol{M}_{R1} + \boldsymbol{M}_{L2}\Delta_M^2\boldsymbol{M}_{R2} + \boldsymbol{M}_{L3}\Delta_M^3\boldsymbol{M}_{R3} \tag{10}$$

where

$$\boldsymbol{M}_{L1} = [\boldsymbol{M}_{11}\ \boldsymbol{M}_{21}\ \cdots\ \boldsymbol{M}_{r1}] \tag{11}$$

$$\Delta_M = \mathrm{diag}(\delta_1\boldsymbol{I}, \delta_2\boldsymbol{I}, \ldots, \delta_r\boldsymbol{I}) \tag{12}$$

$$\boldsymbol{M}_{R1} = [\boldsymbol{I}\ \boldsymbol{I}\ \cdots\ \boldsymbol{I}]^T \tag{13}$$

specify the linear perturbation of the mass matrix due to the variation, and $\boldsymbol{M}_{L2}$, $\boldsymbol{M}_{R2}$, $\boldsymbol{M}_{L3}$, and $\boldsymbol{M}_{R3}$ define quadratic and cubic contributions, with matrices formed accordingly. The size of Δ_M becomes $(n \times r) \times (n \times r)$, with n being the number of degrees of freedom of the finite element model of the aircraft structure. In many practical applications, however, the rank of the perturbation matrices $\boldsymbol{M}_{ij}$ is very low, making Δ_M excessively large, which increases the required computational effort in the robust analysis. To minimize the size of Δ_M, a singular value decomposition of the perturbation matrices can be performed according to

$$\boldsymbol{M}_{ij} = \boldsymbol{U}_{ij}\boldsymbol{\Sigma}_{ij}\boldsymbol{V}_{ij}^T \tag{14}$$

where $\boldsymbol{\Sigma}_{ij}$ is a diagonal matrix of size $\text{rank}(\boldsymbol{M}_{ij})$ containing the singular values of $\boldsymbol{M}_{ij}$. The varying mass matrix can then be written as

$$\boldsymbol{M}(\delta) = \boldsymbol{M}_0 + \boldsymbol{M}_{L1}^{\Sigma}\Delta_1^{\Sigma}\boldsymbol{M}_{R1}^{\Sigma} + \boldsymbol{M}_{L2}^{\Sigma}(\Delta_2^{\Sigma})^2\boldsymbol{M}_{R2}^{\Sigma} + \boldsymbol{M}_{L3}^{\Sigma}(\Delta_3^{\Sigma})^3\boldsymbol{M}_{R3}^{\Sigma} \tag{15}$$

where

$$\boldsymbol{M}_{L1}^{\Sigma} = [\boldsymbol{U}_{11}\boldsymbol{\Sigma}_{11}\ \ \boldsymbol{U}_{21}\boldsymbol{\Sigma}_{21}\ \ \cdots\ \ \boldsymbol{U}_{r1}\boldsymbol{\Sigma}_{r1}] \tag{16}$$

$$\Delta_1^{\Sigma} = \text{diag}(\delta_1\boldsymbol{I}_{\Sigma_{11}}, \delta_2\boldsymbol{I}_{\Sigma_{21}}, \ldots, \delta_r\boldsymbol{I}_{\Sigma_{r1}}) \tag{17}$$

$$\boldsymbol{M}_{R1}^{\Sigma} = [\boldsymbol{V}_{11}\ \ \boldsymbol{V}_{21}\ \ \cdots\ \ \boldsymbol{V}_{r1}] \tag{18}$$

define the decomposed form of the first-order mass uncertainty, and the higher-order contributions $\boldsymbol{M}_{L2}^{\Sigma}$, $\boldsymbol{M}_{R2}^{\Sigma}$, $\boldsymbol{M}_{L3}^{\Sigma}$ and $\boldsymbol{M}_{R3}^{\Sigma}$ are formed accordingly. Note that the uncertainty matrices Δ_i^{Σ} consist of r blocks, but that the size of these blocks in general may be different for different i, depending on the rank of the corresponding perturbation matrix.

To take the varying mass into account in the robust flutter analysis, it is useful to pose the variations in the form of linear fractional transformations (LFTs) [14]. Figure 4 shows the varying mass matrix $\boldsymbol{M}(\delta)$, mapping structural accelerations a to the inertial forces f_M, and the equivalent LFT.

The mapping can be interpreted as a variable matrix $\boldsymbol{M}(\delta)$ from accelerations to inertial forces and is equivalent to the varying mass matrix. From Eq. (15), the matrices Δ_M^{Σ} and $\boldsymbol{P}_M$ are derived:

$$\boldsymbol{P}_M = \begin{bmatrix} 0 & 0 & 0 & 0 & 0 & 0 & \boldsymbol{M}_{R3}^{\Sigma} \\ 1 & 0 & 0 & 0 & 0 & 0 & 0 \\ 0 & 1 & 0 & 0 & 0 & 0 & 0 \\ 0 & 0 & 0 & 0 & 0 & 0 & \boldsymbol{M}_{R2}^{\Sigma} \\ 0 & 0 & 0 & 1 & 0 & 0 & 0 \\ 0 & 0 & 0 & 0 & 0 & 0 & \boldsymbol{M}_{R1}^{\Sigma} \\ 0 & 0 & \boldsymbol{M}_{L3}^{\Sigma} & 0 & \boldsymbol{M}_{L2}^{\Sigma} & \boldsymbol{M}_{L1}^{\Sigma} & \boldsymbol{M}_0 \end{bmatrix} \tag{19}$$

$$\Delta_M^{\Sigma} = \text{diag}\left(\Delta_3^{\Sigma}, \Delta_3^{\Sigma}, \Delta_3^{\Sigma}, \Delta_2^{\Sigma}, \Delta_2^{\Sigma}, \Delta_1^{\Sigma}\right) \tag{20}$$

which shows that the higher-order variations $(\Delta_M^{\Sigma})^2$ and $(\Delta_M^{\Sigma})^3$ are replaced by a linear variation of larger size. This can be done regardless of the order of the polynomial in Eq. (15), and higher-order descriptions of Eqs. (1) and (2) will simply increase the size of Δ_M^{Σ}. The mapping from a to f_M can now be written as

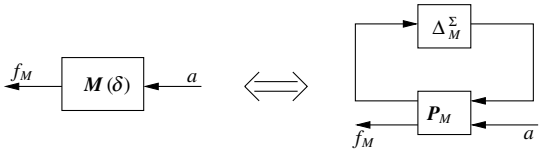

Fig. 4 Equivalent LFT description for $\boldsymbol{M}$.

$$f_M = \boldsymbol{M}(\delta)a = \mathcal{F}_u[\boldsymbol{P}_M, \Delta_M^{\Sigma}j]a \tag{21}$$

where $\mathcal{F}_u[\boldsymbol{P}_M, \Delta_M^{\Sigma}]$ denotes the upper linear fractional transformation, shown in Fig. 4. This form of the variation can now be exploited for assembly of the total system to perform robust analysis.

Robust Analysis

The uncertain flutter equation accounting for parametric variations in the system matrices can generally be written as a nonlinear eigenvalue problem:

$$[\boldsymbol{M}(\delta_M)p^2 + (L^2/V^2)\boldsymbol{K}(\delta_K) - (\rho L^2/2)\boldsymbol{Q}(\delta_Q, p)]v = 0 \tag{22}$$

where $p = g + ik$ is the complex eigenvalue with damping g and reduced frequency k, and v is the eigenvector. The reference length is L, and the airspeed and air density are denoted as V and ρ, respectively. In general, variations δ_M, δ_K, and δ_Q can be defined for the mass matrix $\boldsymbol{M}$, the stiffness matrix $\boldsymbol{K}$, and the aerodynamic matrix $\boldsymbol{Q}$, respectively.

In the present case, there is no variation in the stiffness matrix $\boldsymbol{K}$. For purely real variations, available solution algorithms may require a computational effort that grows exponentially with the size of the problem [15], making the problem infeasible to solve for practical applications. Furthermore, the robustness margin is not necessarily a continuous function when considering purely real uncertainty blocks only, which is pointed out in [13,16]. The problem can be solved much more efficiently if some complex-valued variation is introduced. This can be accomplished by either introducing some small nonphysical variation or, as done in the present study, by introducing some uncertainty in the aerodynamic loads. Some complex-valued uncertainty according to

$$\boldsymbol{Q} = \boldsymbol{Q}_0 + \boldsymbol{Q}_L\Delta_Q\boldsymbol{Q}_R \tag{23}$$

is defined, where $\boldsymbol{Q}_0$ is the nominal aerodynamic matrix, $\boldsymbol{Q}_L = w_Q\boldsymbol{I}$ contains a real scaling factor $w_Q > 0$, $\Delta_Q = \delta_Q\boldsymbol{I}$ contains the complex-valued uncertainty parameter δ_Q, and $\boldsymbol{Q}_R = \boldsymbol{Q}_0$. The uncertainty corresponds to a uniform perturbation of the aerodynamic forces with $|\delta_Q| \leq 1$, where w_Q bounds the perturbation. In the present study, the uncertainty bound $w_Q = 0.02$ was chosen, corresponding to a uniform perturbation of the pressure coefficients on all aerodynamic panels by 2%. The uncertain aerodynamic matrix can be written as an upper LFT $\mathcal{F}_u[\boldsymbol{P}_Q, \Delta_Q]$, where $\boldsymbol{P}_Q$ is derived as

$$\boldsymbol{P}_Q = \begin{bmatrix} 0 & \boldsymbol{Q}_R \\ \boldsymbol{Q}_L & \boldsymbol{Q}_0 \end{bmatrix} \tag{24}$$

The uncertain flutter equation is then written in the LFT form

$$\{\mathcal{F}_u[\boldsymbol{P}_M, \Delta_M^{\Sigma}]p^2 + (L^2/V^2)\boldsymbol{K} - (\rho L^2/2)\mathcal{F}_u[\boldsymbol{P}_Q(p), \Delta_Q]\}v = 0 \tag{25}$$

which can be posed in the form

$$\mathcal{F}_u[\boldsymbol{P}(p), \Delta]v = 0 \tag{26}$$

using simple LFT operations, with $\Delta = \text{diag}(\Delta_M^{\Sigma}, \Delta_Q)$. With this formulation of the uncertain flutter equation, structured singular value (or μ) analysis can directly be applied to detect the flight condition in which some structured Δ with $\|\Delta\|_2 \leq 1$ enables a critical eigenvalue $p = ik$ at some reduced frequency k [9].

Modal Reduction

The system matrices in Eq. (22) are generally large: in the present test case, about $70,000 \times 70,000$. To reduce the computational effort, modal projection is used. A subset of modal coordinates is introduced according to

$$v = \boldsymbol{Z}\eta \tag{27}$$

where the columns of $\boldsymbol{Z}$ hold structural eigenvectors z_i, and the modal coordinate η_i describes the participation of the ith structural eigenvector. By projection of the flutter equation onto the modal subspace, the size of the eigenvalue problem is reduced to the number of considered eigenmodes m. This number has to be chosen sufficiently large to obtain accurate results, but is usually several orders of magnitude smaller than the number of the degrees of freedom. In addition to reducing the size of the system matrices, modal projection may also reduce the size of the uncertainty description. In particular, in cases in which the rank of the perturbation matrix is larger than the number of considered modes, the modal projection will lead to a minimum block size of the uncertainty matrix Δ, reducing the computational effort of the μ analysis.

A concern in robust analysis with varying structural properties is, however, that the modal base $\boldsymbol{Z}$ depends on these variations. In a previous study [10], the impact of mode-shape variations was investigated, and different ways to account for it were proposed. A summary of these approaches is given next.

Increased modal-base: Mode-shape variations can be accounted for by including mode-shape derivatives with respect to the r variation parameters. The extended modal base can be written as

$$\boldsymbol{Z}_{\text{ext}} = [\boldsymbol{Z} \;\; \boldsymbol{Z}_{\Delta}] \tag{28}$$

$$\boldsymbol{Z}_{\Delta} = [v_{11}v_{12} \;\; \cdots \;\; v_{1r}v_{21}v_{22} \;\; \cdots \;\; v_{2r} \;\; \cdots \;\; v_{m1}v_{m2} \;\; \cdots \;\; v_{mr}] \tag{29}$$

$$v_{ij} = \frac{\partial z_i}{\partial \delta_j} \tag{30}$$

where the eigenvector derivatives v_{ij} are computed as described in [17]. The idea of extending the modal base is to include new vectors that point in the directions in which the mode shapes are perturbed. For example, Fig. 5 shows the sixth eigenmode and its derivative due to fuel-level variation in tank element 1.

Including all possible derivatives in $\boldsymbol{Z}_{\Delta}$, however, may lead to similar vectors in the extended modal base, leading to ill-conditioned projected matrices causing numerical problems. Therefore, only the most relevant vectors in $\boldsymbol{Z}_{\Delta}$ are included. To formulate a criterion for selecting additional vectors, the derivative vectors are first normalized to equal norm, and the orthogonal component $v_{ij}^{\perp}$ of each additional vector v_{ij} with respect to the vectors in the modal base is computed using Gram–Schmidt orthogonalization [18] such that

$$\boldsymbol{Z}^T v_{ij}^{\perp} = 0, \qquad (v_{ij}^{\perp})^T v_{ij}^{\perp} = \gamma_{ij} \tag{31}$$

This ensures that only the perpendicular component of any eigenvector derivative will be added to the existing modal base. As a criterion for selecting the most relevant additional vector, the norm of $v_{ij}^{\perp}$ is considered, and the vector with the largest norm is chosen. Note that it is essential to include one vector at a time and to repeat the orthogonalization and selection to ensure that the included vectors are orthogonal to each other and to the current modal base, and to prevent similar vectors from being included.

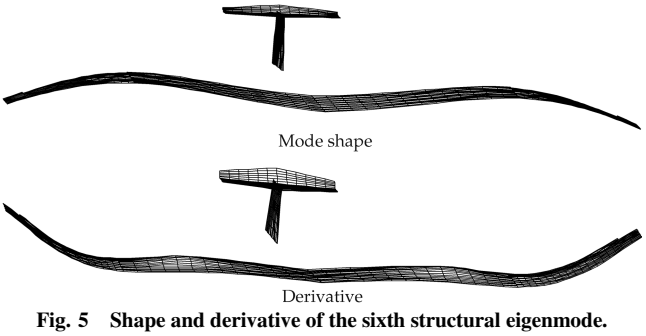

Fig. 5 Shape and derivative of the sixth structural eigenmode.

Iterative modal base: With this approach, the resulting worst-case configuration from the robust analysis is used to compute a new modal base. The new modal base is then used for the modal projection in the analysis. This is done iteratively, until the resulting worst-case perturbation matches the current modal base. The iterations are terminated when two consecutive iterations h and $h+1$ fulfill

$$\|\Delta_M^{\Sigma}(h+1) - \Delta_M^{\Sigma}(h)\|_{\infty} < \epsilon \tag{32}$$

where ϵ is a specified tolerance parameter: in the present study, chosen as 10^{-3}. Although appealing due to preserving a small size of the problem in each iteration, a drawback is that the worst-case perturbation is computed by solving a nonconvex optimization problem, and the global worst-case perturbation is not necessarily found.

Results

To obtain sufficiently accurate results, the first 40 eigenmodes were selected to establish the reduced modal base. Because the critical flutter mechanism is symmetric with respect to the x-z plane, only symmetric modes were considered, thus reducing the modal base to 19 eigenvectors. Nominal p-k flutter analysis [19] of the case with empty tanks gave a flutter speed of $u = 100$ m/s at a frequency $f = 9.4$ Hz. Adding an aerodynamic uncertainty with a bound of $w_Q = 0.02$, the robust flutter speed without mass variations was reduced to $u = 99$ m/s. The aerodynamic uncertainty was then kept at the same level throughout the analysis. Thus, proper robust analysis should yield worst-case flutter speeds of 99 m/s or below. The robust analysis for finding the worst-case flutter speed and the corresponding fuel configuration was performed for two different tank configuration with four tank elements. In addition to configuration A, shown in Fig. 2, configuration B was also investigated.

The robust results for the different tank configurations are summarized in Table 1. The first row summarizes the nominal flutter speed u_{nom} for the different tank configurations in which all tanks are half-filled ($\delta_i = 0$ for all tanks). The robust flutter speed using the original modal base is denoted as u_{rob}, and δ_{wc} is the corresponding worst-case configuration found by the μ analysis that was used to update the modal base for the iterative approach. Results from the iterative algorithm for updating the modal base are included as well, denoted as $\hat{u}_{\text{rob}}$ and $\hat{\delta}_{\text{wc}}$, respectively.

In configuration A, the tanks were distributed inside the wing. The maximum fuel weight of the entire tank was about 60 kg per wing. Note that the weight of the aircraft without fuel and payload was 380 kg. The resulting nominal analysis for $\Delta = 0$ provided a flutter speed of 143 m/s. Using robust analysis, the robust flutter speed was reduced significantly to 105 m/s, along with a worst-case $\delta_i = -1$ for all tank elements, corresponding to an empty tank. This result, however, is not robust with respect to the flutter speed of the empty-tank configuration, which is known to be 99 m/s with the aerodynamic uncertainty. The reason for this was found to be an insufficient modal base. To improve the result, the modal base was adapted to account for mode-shape variations due to structural variations.

Using the iterative approach for computing the perturbed modal base provided correct results, and a robust flutter speed of 96 m/s was obtained. Because the worst-case perturbation was equal to -1 for all tanks in both the first and the second iterations, the iterative

Table 1 Robust flutter results

	Config. A	Config. B
u_{nom}	143 m/s	109 m/s
u_{rob}	105 m/s	102 m/s
δ_{wc}	$[-1,-1,-1,-1]$	$[-1,-1,-1,0.22]$
$\hat{u}_{\text{rob}}$	96 m/s	97 m/s
$\hat{\delta}_{\text{wc}}$	$[-1,-1,-1,-1]$	$[-1,-1,-1,0.22]$

approach had converged according to Eq. (32) after one step. The obtained robust flutter speed was slightly conservative with respect to the known flutter speed of 99 m/s, the reason for this being the fact that the μ-k algorithm is based on an upper-bound estimation of the μ value to guarantee robustness.

In configuration B, a slender tank with a total fuel weight of 16 kg per half-wing was considered. For the tank configuration B shown in Fig. 2, the nominal flutter speed was 109 m/s. Using the robust analysis, the flutter speed was reduced to 102 m/s with the original modal base, along with a worst-case perturbation corresponding to a fuel distribution in which only the rear tank element is filled. Again, this result is not robust, the reason being an incorrect modal base.

For this tank configuration, it appeared that there is a fuel configuration that is worse than empty tanks. Further, it was found that the resulting worst-case perturbation is dependent on the tools used for computing the μ value. In general, the μ value cannot be evaluated exactly and has to be estimated by upper and lower bounds [13]. Figure 6 shows the upper and lower bounds of μ as a function of the reduced frequency k for some given airspeed for configuration B.

The lower bound corresponds to some Δ found by optimization and corresponds to the exact μ value if the global optimum has been found. Because this cannot be guaranteed, however, the upper bound must be considered to guarantee robustness with respect to the uncertainty parameters. In μ-k flutter analysis, the upper-bound peak is considered, and robust stability for some given airspeed is guaranteed when the peak is below one. An obvious problem appears when the upper and lower bounds differ significantly. In the present case, the peaks appear at different frequencies. According to the iterative algorithm, the worst-case perturbation is to be computed at the reduced frequency k_{rob} of the upper-bound peak, leading to a perturbation that is not worst-case according to the lower bound. Also for this tank configuration, one outer iteration was required to make the iterative approach converge. For both configurations, it was found that the worst-case perturbation was less sensitive to an incorrect modal base than the related flutter speed, therefore making the iterative approach converge in one step only.

A number of nominal flutter analyses were performed for different filling levels of the rear tank, and it was found that a full rear tank in fact leads to the lowest flutter speed at 98 m/s with aerodynamic uncertainty, thus confirming the prediction of the lower-bound graph. Despite this, the modal base was updated according to the iterative algorithm using the perturbation corresponding to the frequency of the upper-bound peak, and it was found that the perturbation is close enough to the worst-case perturbation and that the modal base was perturbed sufficiently to yield robust results. The resulting robust flutter speed of 97 m/s is slightly conservative with respect to the flutter speed found by the nominal analysis, with a filled rear tank at 98 m/s.

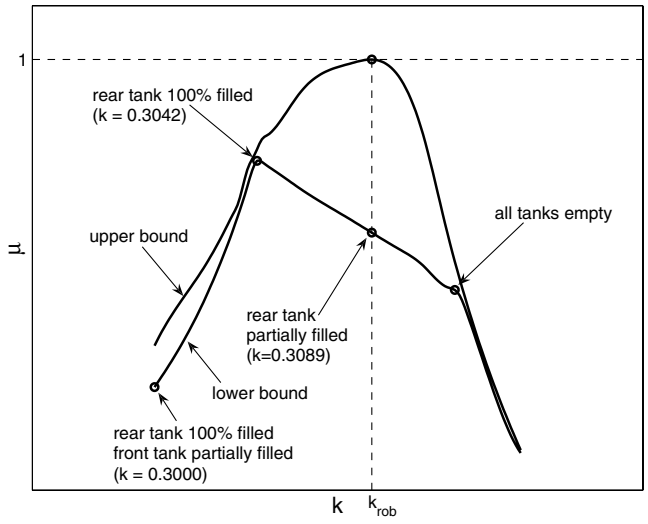

Fig. 6 Upper and lower bounds of frequency-dependent μ value.

Increased modal base: It was found that increasing the modal base by mode-shape derivatives did not perturb the modal base sufficiently to obtain correct results in the robust analysis. One of the main problems when including mode-shape derivatives is that the computation of mode-shape derivatives is computationally expensive for a realistic aircraft model with a large number of degrees of freedom. In addition, it is not obvious which derivatives should be included in the modal base to adapt the modal base to the perturbed structure without making the projected system matrices ill-conditioned.

Finally, it was also found that simply increasing the size of the modal base did not improve results very much. This may be obvious, because the perturbation does typically not disturb the structural mode shapes in a way that can be captured by a moderate number of additional eigenmodes.

For both approaches considering an increased modal base, the robust flutter speed was not changed significantly, compared with the robust analysis based on the nominal modal base.

Computational effort: The most significant computational effort is spent on solving the μ problem based on Eq. (26), and the solution time was found to depend cubically on the size of Δ. As discussed earlier, the minimum size of the structured uncertainty for each uncertainty parameter is either the number of modes or the rank of the perturbation matrix. In the present case, the rank of the perturbation matrices was 12 or less in all considered cases, whereas the number of modes used in the analysis was 19. Increasing the number of modes by mode-shape derivatives therefore had no significant impact on the computational effort needed for solving the μ problem. In the present case, one μ evaluation with four variation parameters took approximately 10 s on a 2.5-GHz Pentium computer. Note that the computational effort generally depends on the size of the structural (real-valued) uncertainties, and the size of the aerodynamic (complex-valued) uncertainty in the present study does not have any significant impact, due to its simplicity. Depending on the algorithm used for bounding the μ peak, up to 100 evaluations may be required to solve the robust flutter problem for one mode.

Conclusions

It was shown that robust flutter analysis can be used for assessing the influence of fuel variations on the flutter boundary. The presented approach is more efficient than considering different configurations by hand and guarantees robustness with respect to the flutter speed for all possible configurations. From investigations with different fuel-tank geometries and discretizations, it was found that there may be worst-case configurations that cannot be captured when modeling the fuel level in the entire tank using one parameter only.

Although it is a secondary effect in terms of the impact on the flutter speed, the variation of the structural mode shapes due to fuel variations can play a significant role. In the present case, the flutter speed was overestimated when neglecting this effect. Including eigenmode derivatives with respect to the uncertainty for extending the modal base seems insufficient and is computationally expensive when mode-shape derivatives of complex aircraft structures have to be computed. Using an iterative base yields good results at less computational effort, but there is no guarantee for convergence of the iteration. The obtained solution can, however, be judged by considering the upper and lower bounds of the obtained μ value to increase the reliability of the robust boundary.

This study also demonstrated that commercial analysis tools such as Nastran can efficiently be used to generate the database needed to perform robust flutter analysis considering structural variations. Because these tools are frequently used in aircraft design and certification analysis, numerical models of the nominal configurations often exist, making robust analysis accessible with modest additional modeling effort.

The μ-k algorithm is also efficient in terms of exploiting nominal flutter results, because the frequency of the nominal mode can be used as an initial guess when bounding the peak in the μ-k graph. When large structural variations are present, however, finding the critical peak is more difficult, because the peak location may deviate

significantly from the nominal frequency, due to the impact of the variations on the structural eigenfrequencies. In addition, the critical flutter mechanism may change, making it necessary to perform a robust flutter analysis of several modes.

Acknowledgments

This work was financially supported by the Swedish Defence Material Administration (FMV) under contract 278294-LB664174 and the National Program for Aeronautics Research (NFFP).

References

[1] Zhou, K., and Doyle, J. C., *Essentials of Robust Control*, Prentice–Hall, Upper Saddle River, NJ, 1998.

[2] Lind, R., and Brenner, M., *Robust Aeroservoelastic Stability Analysis*, Springer–Verlag, London, 1999.

[3] Lind, R., "Match-Point Solutions for Robust Flutter Analysis," *Journal of Aircraft*, Vol. 39, No. 1, 2002, pp. 91–99.

[4] Danowsky, B., Chavez, F., and Brenner, M., "Formulation of an Aircraft Structural Uncertainty Model for Robust Flutter Predictions," 45th AIAA/ASME/ASCE/AHS/ASC Structures, Structural Dynamics and Materials Conference, Palm Springs, CA, AIAA Paper 2004-1853, 2004.

[5] Karpel, M., Moulin, B., and Idan, M., "Robust Aeroservoelastic Design with Structural Variations and Modeling Uncertainties," *Journal of Aircraft*, Vol. 40, No. 5, 2003, pp. 946–954.

[6] Moulin, B., "Modeling of Aeroservoelastic Systems with Structural and Aerodynamic Variations," *AIAA Journal*, Vol. 43, No. 12, 2005, pp. 2503–2513.

[7] Borglund, D., "The μ-*k* Method for Robust Flutter Solutions," *Journal of Aircraft*, Vol. 41, No. 5, 2004, pp. 1209–1216.

[8] Borglund, D., "Upper Bound Flutter Speed Estimation Using the μ-*k* Method," *Journal of Aircraft*, Vol. 42, No. 2, 2005, pp. 555–557.

[9] Borglund, D., and Ringertz, U., "Efficient Computation of Robust Flutter Boundaries Using the μ-*k* Method," *Journal of Aircraft*, Vol. 43, No. 6, 2006, pp. 1763–1769.

[10] Heinze, S., and Borglund, D., "Robust Flutter Analysis Considering Modeshape Variations," Department of Aeronautical and Vehicle Engineering, Royal Inst. of Technology (KTH), TR Trita-AVE 2007:27, Stockholm, Sweden, 2007.

[11] Eller, D., and Ringertz, U., "Aeroelastic Simulations of a Sailplane," Department of Aeronautical and Vehicle Engineering, Royal Inst. of Technology (KTH), TR Trita-AVE 2005:41, Stockholm, Sweden, 2005.

[12] "MSC.Nastran 2004 Reference Manual," MSC Software Corp., Santa Ana, CA, 2004.

[13] Balas, G. J., Doyle, J. C., Glover, K., Packard, A., and Smith, R., μ-*Analysis and Synthesis Toolbox for Use with MATLAB*, MathWorks, Inc., Natick, MA, 1995.

[14] Doyle, J. C., Packard, A., and Zhou, K., "Review of LFTs, LMIs, and ,μ," *Proceedings of the 30th IEEE Conference on Decision and Control*, Inst. of Electrical and Electronics Engineers, New York, Dec. 1991, pp. 1227–1232.

[15] Hayes, M. J., Bates, D. G., and Postlethwaite, I., "New Tools for Computing Tight Bounds on the Real Structured Singular Value," *Journal of Guidance, Control, and Dynamics*, Vol. 24, No. 6, 2001, pp. 1204–1213.

[16] Barmish, B. R., Khargonekar, P. P., Shi, Z. C., and Tempo, R., "Robustness Margins Need Not be a Continuous Function of the Problem Data," *Systems & Control Letters*, Vol. 15, No. 2, Aug. 1990, pp. 91–98.

[17] Ringertz, U. T., "On Structural Optimization with Aeroelastic Constraints," *Structural Optimization*, Vol. 8, No. 1, 1994, pp. 16–23.

[18] Golub, G. H., and van Loan, C. F., *Matrix Computations*, 3rd ed., Johns Hopkins Univ. Press, Baltimore, MD, 1996.

[19] Bäck, P., and Ringertz, U. T., "Convergence of Methods for Nonlinear Eigenvalue Problems," *AIAA Journal*, Vol. 35, No. 6, 1997, pp. 1084–1087.